Ancient trans-acting siRNAs modulate auxin sensitivity in the moss *Physcomitrella patens*

Yevgeniy Plavskin[1,2], Akitomo Nagashima[3,4], Pierre-François Perroud[5,6], Gurinder S. Atwal[1], Mitsuyasu Hasebe[3,4], Ralph S. Quatrano[5], Marja C.P. Timmermans[1,7]

1. Watson School of Biological Sciences, Cold Spring Harbor Laboratory, Cold Spring Harbor, NY, USA
2. Present address: Department of Biology, NYU Center for Genomics and Systems Biology, New York, NY, USA
3. National Institute for Basic Biology, Okazaki 444-8585, Japan
4. Exploratory Research for Advanced Technology, Japan Science and Technology Agency, Okazaki 444-8585, Japan
5. Department of Biology, Washington University, St. Louis, MO, USA
6. Present address: Philipps-Universität Marburg, FB Biologie, Zellbiologie II, Marburg, Germany
7. Center for Plant Molecular Biology, University of Tübingen, Tübingen, Germany

Author of Correspondence: Marja Timmermans
1 Bungtown Road
Cold Spring Harbor
NY 11724
e-mail: timmerma@cshl.edu
phone: (516) 367-8835
fax: (516) 367-8369

Running Title: Modulation of the moss auxin response by tasiRNAs

Keywords: small RNA, evolution, gene regulatory network, auxin, Physcomitrella

ABSTRACT

Novel developmental programs often evolve via the cooption of existing genetic networks. To gain insight into this evolutionary process, we explored an independent cooption event of the *TAS3* tasiRNA pathway, which has been repeatedly redeployed over the course of plant evolution, in the moss *Physcomitrella patens*. We find an ancestral role for this pathway in the spatial regulation of a conserved set of Auxin Response Factors. In moss, this results in stochastic patterning of the filamentous protonemal tissue. Through a combination of computational modeling and experimentation, we demonstrate that tasiRNA regulation confers sensitivity and robustness onto the auxin response. The loss of auxin sensitivity is paralleled by decreased developmental sensitivity to nitrogen, a key environmental signal. We propose that the properties lent to the auxin response gene regulatory network by tasiRNAs, along with their ability to stochastically modulate development in response to environmental cues, have contributed to the tasiRNA-ARF module's repeated cooption over the course of plant evolution.

INTRODUCTION

The evolution of novel forms is frequently driven by the cooption of existing developmental gene regulatory networks (GRNs) (Erwin and Davidson, 2009). Certain networks appear especially prone to such evolutionary repurposing, leading to the regulation of multiple diverse developmental processes by a single conserved GRN (Carroll et al., 2004a; Plavskin and Timmermans, 2012). The properties that favor the recurring cooption of some GRNs remain largely unknown. One possibility is that frequently coopted GRNs regulate defined cellular processes, allowing the evolutionary redeployment of such 'differentiation modules' in a new context (Erwin and Davidson, 2009). On the other hand, it has been postulated that small network motifs may have been repeatedly reutilized by evolution to regulate diverse processes because of their signaling properties (Martinez et al., 2008; Milo et al., 2002).

The mechanism of network cooption has been the subject of extensive investigation, with changes impacting the expression of central GRN components frequently driving the evolution

of developmental novelties (Carroll et al., 2004b). Small regulatory RNAs, which play a key role in gene regulation during development in both plants and animals, are one mechanism for driving such evolutionary change (Plavskin and Timmermans, 2012). In addition to regulating the level and spatiotemporal expression pattern of their targets, small RNAs are thought to reduce the inherent noisiness of transcription or, as an outcome of mobility, give rise to sharpened gene expression boundaries (Chitwood et al., 2009; Levine et al., 2007; Schmiedel et al., 2015; Skopelitis et al., 2012). These properties may lend robustness to small RNA-regulated networks, perhaps influencing GRN cooptability. An understanding of how the developmental roles of small RNAs and their targets change over the course of evolution may therefore lead to important insights regarding the properties of GRNs that promote their repeated evolutionary cooption (Plavskin and Timmermans, 2012).

Plants have undergone tremendous diversification since their colonization of land ~450 million years ago (Kenrick and Crane, 1997). Some notable innovations include the formation of a lignified vasculature, a sporophyte-dominant life cycle, layered meristems, leaves, flowers, fruits, and seed. While these changes in body plan occurred in parallel with repeated losses and gains of developmentally important small RNAs, select small RNA families and their targets have remained conserved since the most recent common ancestor of all land plants (Axtell et al., 2007; Cuperus et al., 2011).The *TAS3* trans-acting short interfering RNA (tasiRNA) pathway is in this regard of special interest: while it is conserved throughout land plant evolution, its contributions to development vary extensively even among flowering plants (Plavskin and Timmermans, 2012). *TAS3* tasiRNA biogenesis is triggered in response to the miR390-directed cleavage of a set of non-coding *TAS3* transcripts, which causes conversion of these precursors into long double-stranded RNAs (dsRNAs) by RNA-DEPENDENT RNA POLYMERASE 6 (RDR6) and SUPPRESSOR OF GENE SILENCING 3 (SGS3). The dsRNA intermediates are subsequently processed by DICER-LIKE 4 (DCL4) into 21-nt tasiRNAs that are phased to yield discrete small RNA species. A subset of these tasiRNAs are biologically active and, like miRNAs, act at the post-transcriptional level to regulate expression of specific gene targets (reviewed in Chapman and Carrington (2007)).

Although related tasiRNA biogenesis pathways initiated by other miRNAs exist (Fei et al., 2013), only the miR390-dependent *TAS3* tasiRNA pathway is conserved across land plant evolution (Axtell et al., 2007). Furthermore, only the *TAS3* tasiRNAs have demonstrated roles in development. The *TAS3*-derived tasiARFs, which regulate the expression of *AUXIN RESPONSE FACTORS* within the *ARF3* and *ARF4* clade, function in the specification of adaxial-abaxial (top-bottom) leaf polarity in a number of flowering plant species, including *Arabidopsis*, tomato, rice, and maize (Chitwood et al., 2009; Nagasaki et al., 2007; Nogueira et al., 2007; Yifhar et al., 2012). In addition, these tasiRNAs play a key role in monocot shoot meristem maintenance (Dotto et al., 2014; Nagasaki et al., 2007), contribute to heteroblasty and lateral root outgrowth in *Arabidopsis* (Hunter et al., 2003; 2006; Marin et al., 2010; Yoon et al., 2010), and regulate leaf complexity and lobing in *Lotus* and *Medicago*, respectively (Yan et al., 2010; Zhou et al., 2013). Thus, even within the flowering plant lineage, the *TAS3* tasiRNA pathway has been coopted for the regulation of diverse developmental processes.

Moreover, the organs whose development is regulated by *TAS3* tasiRNAs in flowering plants - leaves, roots, and layered shoot meristems - evolved long after the pathway itself did (Axtell and Bartel, 2005; Kenrick and Crane, 1997). The genome of the moss *Physcomitrella patens*, which last shared a common ancestor with flowering plants ~450 million years ago, includes six *TAS3* loci (Arif et al., 2012; Axtell et al., 2007). As in flowering plants, a subset of *TAS3*-derived tasiRNAs in moss target transcripts of ARF transcription factors (Axtell et al., 2007; Talmor-Neiman et al., 2006). This suggests an additional, yet unknown role of *TAS3*-derived tasiRNAs in ancient land plant development. Studying the role of these small RNAs outside the flowering plant lineage thus presents a unique opportunity to shed light on potential ancestral functions of this pathway, and to explore the properties that have led to this pathway's repeated cooption over the course of plant evolution.

To this end, we generated mutants in the moss *Physcomitrella patens* that lack SGS3 activity and are impaired in tasiRNA biogenesis. The *Ppsgs3* mutants exhibit defects in gametophore formation, protonemal branching, and differentiation of specialized caulonemal filaments resulting from the upregulation of a conserved set of repressor *ARF* genes at the edge of the

developing protonema. We show that tasiRNAs act to generate differential levels of *ARF* expression at the protonemal edge, leading to stochastic patterning of protonemal cell fate determination. Through a combination of computational modeling and experimentation, we further demonstrate that tasiRNA regulation confers sensitivity and robustness onto the auxin response. Finally, we find that *Physcomitrella* plants defective in tasiRNA biogenesis display decreased developmental sensitivity to a key environmental signal, in line with this pathway's role in tuning the auxin sensitivity of cells at the plant's growing edge. We propose that the properties lent to the auxin response gene regulatory network by tasiRNAs, along with their ability to stochastically modulate development in response to environmental cues, have contributed to the repeated cooption of the tasiRNA-ARF module over the course of plant evolution.

RESULTS

Disruption of tasiRNA biogenesis in *Physcomitrella* impairs protonemal development

Physcomitrella homologs of *RDR6* and *DCL4* with a conserved role in tasiRNA biogenesis have been described previously (Cho et al., 2008; Talmor-Neiman et al., 2006). However, the contributions of tasiRNAs to moss development remain unresolved, in part because mutations perturbing these biogenesis components give rise to disparate phenotypes. To gain insight into the developmental role of the *TAS3* tasiRNA pathway outside the flowering plant lineage, we used targeted recombination to disrupt the single *Physcomitrella* homolog of *SGS3*, *PpSGS3* (**Figure S1A-E, Table S1**). Consistent with a conserved role of PpSGS3 in tasiRNA biogenesis, levels of these small RNAs are drastically reduced in *Ppsgs3* mutants (**Figure 1A**). The *Physcomitrella* genome includes six *TAS3* loci, *PpTAS3a-f*. These, in contrast to their counterparts in flowering plants, yield two sets of biologically active small RNAs: tasiARF, which target transcripts of four *ARF* genes, *PpARFb1-4*, and tasiAP2, which regulate expression of members in the APETALA2 (AP2) transcription factor family (Arif et al., 2012; Axtell et al., 2007; Talmor-Neiman et al., 2006). Levels of both biologically active tasiRNAs are drastically reduced in *Ppsgs3* mutants, whereas levels of miR390, which functions upstream of SGS3 in tasiRNA biogenesis, remain unaffected (**Figure 1A**). In addition, the tasiRNA-guided cleavage

of target transcripts is specifically affected in *Ppsgs3*. Expression of the *PpARFb* genes is regulated by tasiARF as well as the miRNA miR1219 (Axtell et al., 2007). 5' RACE analysis revealed that while the miR1219-guided cleavage of *PpARFb1* and *PpARFb4* transcripts is not noticeably affected, the accumulation of tasiRNA-directed cleavage products for both transcripts is strongly reduced in *Ppsgs3* plants (**Figure S2A**). Together with the striking reduction in tasiRNA levels in *Ppsgs3*, this indicates that a role of SGS3 in tasiRNA biogenesis is conserved across land plants.

Loss of PpSGS3 activity results in defined developmental defects. While *Ppsgs3* plants show no obvious sporophyte defects and produce viable spores (**Figure S2D, E**), protonemal development in the mutant is perturbed. Following germination, wild type moss spores produce filamentous, branching protonema comprised initially of chloroplast-rich chloronema. However, as development progresses, or in response to certain environmental cues, dividing chloronemal cells may transition to give rise to the more elongated caulonemal cells. In addition, modified protonemal side branches also give rise to buds, which in turn develop into leafy gametophores (Reski, 1998). While indistinguishable from wild type early in development, the chloronemal networks of 15-day-old *Ppsgs3* mutants are smaller and denser than those of wild type (**Figure 1B, C**). These phenotypes appear to result in part from a decrease in cell size, as chloronemal cells in *Ppsgs3* plants are reduced in length by approximately 6% compared to wild type (**Figure 1D**). In addition, the chloronemal filaments in *Ppsgs3* show a more complex branching pattern (**Figure 1E, F; S2B, C**). Wild type protonemal branching largely follows a stereotyped pattern, in which a 'main filament' extending from the center of the plant to its periphery produces one or occasionally two branches at nearly every cell (**Figure 1E**). In addition, a subset of cells along these primary branches form secondary branches. However, tertiary branches are rarely observed, demonstrating that protonemal branching is effectively determinate. In contrast, *Ppsgs3* protonemal filaments consistently show higher order branching patterns compared to wild type protonema of a similar age (**Figure 1F; S2C**). Both the number of secondary branches and their length, measured as the number of cells per branch, are variably increased in *Ppsgs3*. Likewise, the number and length of tertiary branches is increased, and quaternary branches regularly occur near the center of 20 day-old *Ppsgs3* plants. These data suggest that loss of SGS3 activity and tasiRNA biogenesis causes a decrease in both chloronemal cell size and branch

determinacy.

The most striking phenotype of *Ppsgs3* mutants, however, concerns the formation of long caulonemal filaments. Under the growth conditions used, long caulonemal filaments visibly extend from the chloronemal edge of wild type plants after approximately two weeks of development, causing older plants to take on a fuzzy appearance (**Figure 1B**). Although cells with diagonal cross-walls reminiscent of caulonema are occasionally observed in the protonemal network of *Ppsgs3* plants, these mutants either completely lack long caulonemal filaments, or rarely form small isolated patches of such filaments along the otherwise smooth protonemal edge (**Figure 1B, C**). Even after two months of growth, *Ppsgs3* plants rarely form long caulonemal filaments, indicating a suppression of caulonemal filament formation rather than a delay in the chloronema-to-caulonema transition upon loss of SGS3 function.

In addition to these protonemal phenotypes, *Ppsgs3* plants form significantly fewer leafy gametophores than wild type (**Figure 1G**), although gametophore morphology itself is normal (**Figure S2F-I**). This defect is not fully explained by the lack of long caulonemal filaments in *Ppsgs3* mutants, as a significant decrease in gametophore number is detected prior to the normal appearance of these filaments at ~15 days of growth. Indeed, gametophores in *Physcomitrella* also develop from chloronema (Menand et al., 2007a). Their reduced numbers indicate a role for PpSGS3 in gametophore formation as well as protonemal development. While a reduction in caulonema formation has also been reported for *Pprdr6* mutants, the observed decrease in gametophore number in *Ppsgs3* is at odds with previous findings showing that *Pprdr6* plants develop more gametophores than wild type (Cho et al., 2008; Talmor-Neiman et al., 2006). Potential roles of *PpRDR6* outside of tasiRNA biogenesis may account for this difference. PpRDR6 shares a role with PpDCL3 in the production of 22-24 nt siRNAs, and similar to *Pprdr6,* gametophore production in *Ppdcl3* is accelerated (Cho et al., 2008). As *Ppdcl3* does not affect tasiRNA biogenesis, a loss of 22-24 nt siRNAs, rather than the loss of tasiRNAs, may account for the accelerated gametophore formation in *Pprdr6* as in *Ppdcl3*.

Taken together, our results indicate that a role for SGS3 in tasiRNA biogenesis is conserved between *Physcomitrella* and flowering plants. PpSGS3 is required for normal gametophyte

development, with *Ppsgs3* mutants displaying defects in chloronemal cell size and branch determinacy, caulonemal differentiation, and gametophore formation.

tasiRNAs affect gametophyte development by regulating expression of *PpARFb* genes

In flowering plants, tasiRNAs exert their effect on development by regulating expression of ARF3 and ARF4 transcription factors (Chitwood et al., 2009; Dotto et al., 2014; Hunter et al., 2006; Song et al., 2012; Yifhar et al., 2012; Zhou et al., 2013). In *Physcomitrella*, *TAS3*-derived tasiRNAs similarly target *ARF* transcripts, and in addition have a unique set of targets in the AP2 transcription factor family (Axtell et al., 2007; Talmor-Neiman et al., 2006). Moreover, an apparent species-specific *TAS* pathway exists in moss. The *Physcomitrella* genome includes *TAS* loci whose transcripts are processed in a miR156- and miR529-dependent manner, referred to as *TAS6,* which yield tasiRNAs targeting a ZF-domain transcription factor (Arif et al., 2012; Cho et al., 2012). To elucidate which tasiRNA targets are responsible for the developmental defects observed in *Ppsgs3* mutants, we compared the expression levels of known tasiRNA targets between wild type and *Ppsgs3* in 15-day-old plants, when all aspects of the *Ppsgs3* phenotype are apparent. Of the four tasiARF-regulated *ARF* genes in *Physcomitrella*, only *PpARFb1*, *PpARFb2*, and *PpARFb4* are expressed during the gametophyte stage of development (Rensing et al., 2005). In *Ppsgs3* plants, transcript levels of all three *ARF* genes are upregulated ~2- to 3-fold relative to wild type (**Figure 2A**). In contrast, expression levels of the tasiAP2 and tasiZF targets are not significantly changed between wild type and *Ppsgs3* at this developmental stage (**Figure 2A**). The observed increase in *PpARFb1*, *PpARFb2*, and *PpARFb4* transcript levels suggests that the *Ppsgs3* developmental defects result, at least in part, from a failure to correctly regulate these tasiARF targets.

To investigate this hypothesis, we generated plants that allow the estradiol-inducible expression of HA-tagged, miR1219- and tasiARF-resistant (m*t*) versions of *PpARFb2* and *PpARFb4* (Kubo et al., 2013; **Figure S3A, B**), which represent the two distinct branches of the *PpARFb* clade (Plavskin and Timmermans, 2012). Even when grown on low concentrations of estradiol, the phenotype of plants overexpressing *PpARFb2-m*t** or *PpARFb4-m*t** resembles that of *Ppsgs3*. Such plants form denser protonema with fewer gametophores and suppress the transition

from chloronemal to caulonemal development (**Figure S3C-I**). Similar phenotypes are not observed in plants expressing a GUS-GFP fusion protein upon estradiol treatment (**Figure S3C, D**). This indicates that PpARFb2 or PpARFb4 overexpression is sufficient to recapitulate the *Ppsgs3* phenotype, which lends support to the hypothesis that loss of tasiARF activity and the correct regulation of its *PpARFb* targets underlies the developmental defects of *Ppsgs3* mutants. In addition, this finding reinforces the notion that a defect in the biogenesis of small RNAs other than the tasiRNAs accounts for the increased gametophore numbers in *Pprdr6* (Cho et al., 2008; Talmor-Neiman et al., 2006).

To substantiate the above findings and to explore the interaction between tasiARFs and miR1219 in the regulation of *PpARFb* expression, we generated a translational fusion of the endogenous *PpARFb4* gene to the GUS reporter, and introduced mutations that prevent targeting of *PpARFb4-GUS* transcripts by miR1219 (*m**), tasiARF (*t**), or both small RNAs (*m*t**) (**Figure S4A-E, Table S1**). *PpARFb4* was chosen because its expression is especially sensitive to changes in tasiARF regulation **(Figure 2A; S2A)**. *PpARFb4-GUS* plants show a subtle decrease in the number of caulonemal filaments but otherwise look phenotypically normal (**Figure 2B**). Likewise, plants expressing the *PpARFb4-GUS-m** or *PpARFb4-GUS-t** variants show a variable decrease in the number of long caulonema; however, neither fully recapitulates the *Ppsgs3* phenotype (**Figure 2C, D)**. Thus, even though *PpARFb4* transcript levels are increased approximately 3-fold in *Ppsgs3*, loss of tasiARF-mediated regulation of *PpARFb4* alone is insufficient to recapitulate the *Ppsgs3* phenotype. This suggests that altered expression of multiple *PpARFb* targets is needed to condition the developmental defects observed in *Ppsgs3*. Indeed, the phenotypic similarities between *PpARFb2-m*t** and *PpARFb4-m*t** overexpressing plants (**Figure S3E-H**) indicates that proteins within this clade have related activities.

Importantly, *PpARFb4-GUS-m*t** plants fail to form long caulonemal filaments (**Figure 2E**), closely mimicking the phenotype observed in *Ppsgs3*. Likewise, *PpARFb4-GUS-m*t** mutants show a significant and very strong decrease in gametophore number, with the onset of gametophore formation delayed approximately one week relative to plants expressing the small RNA-sensitive *PpARFb4-GUS* fusion (**Figure 2F**). These results indicate that tasiARF and miR1219 coordinately regulate *PpARFb4* expression during gametophyte development.

Moreover, the phenotype of *Ppsgs3* mutants, in which expression of three *PpARFb* genes is increased due to loss of tasiARF activity, can be phenocopied by perturbation of tasiARF and miR1219 regulation of *PpARFb4* alone, as well as by the inducible overexpression of a similar mutant version of *PpARFb2* (**Figure S3E, F**). It follows that tasiARF, in concert with miR1219, regulates the chloronema-to-caulonema transition and gametophore formation in *Physcomitrella* by fine-tuning the combined level of *PpARFb* expression. When *PpARFb* levels overall exceed a certain level, not reached in *PpARFb4-GUS-t** plants, formation of long caulonemal filaments and gametophores is inhibited.

tasiARF and miR1219 limit PpARFb4 expression at the protonemal edge

Small RNAs have diverse contributions to plant development (reviewed in Benkovics and Timmermans (2014) and Skopelitis et al. (2012)). Small RNAs are thought to refine levels of protein accumulation by dampening the noise in target gene expression, and can limit expression of their developmental targets to defined spatial and/or temporal domains. Considering that the formation of caulonema and leafy gametophores is in part temporally regulated (Bopp, 1980), tasiARF and miR1219 might control the development of these tissues by regulating the temporal window of *PpARFb* expression. This possibility seems intriguing, as tasiRNAs in *Arabidopsis* are known to regulate developmental timing by delaying the expression of adult leaf traits (Hunter et al., 2006). To assess the possibility that tasiARF and miR1219 exert their effects by regulating the timed repression of *PpARFb* activity, we monitored their accumulation over 3 weeks of gametophyte growth. Protonemal tissue grown on cellophane plates is commonly used to quantify transcript abundance in moss (for example, see Arif et al. (2012); Cho et al. (2008); Pires et al. (2013)), however, such growth conditions substantially impact gene expression levels (**Figure S5A, B**). Therefore, target gene expression was assayed in intact plants grown under the same conditions used for phenotypic analysis. While expression levels for tasiARF, miR1219, and miR390 are temporally regulated and increase up to ~60 fold during that developmental time window (**Figure S5A**), transcript levels for *PpARFb1, PpARFb2*, and *PpARFb4* change comparatively little during that time (**Figure S5B**).

This observation argues against a role for tasiARF and miR1219 solely in the temporal regulation of *PpARFb* genes, and instead suggests that these small RNAs may act to maintain a

spatial domain of *PpARFb* expression. To examine this possibility, we compared the pattern of PpARFb4-GUS activity in plants expressing the wild type or small RNA-resistant variants of this reporter. When regulated by tasiARF and miR1219, *PpARFb4-GUS* expression is limited to 1-3 cells nearest the filament tip at the outer edge of the protonema. Expression in these cells is punctate, consistent with PpARFb proteins functioning as nuclear-localized transcription factors (**Figure 2G**). Interestingly, *PpARFb4-GUS* expression is not seen in all chloronemal filaments, but instead appears patchy, with a subset of filaments along the circumference of the plant showing reporter activity. Considering that increased *PpARFb* expression represses caulonemal filament formation, stochasticity in PpARFb4 levels along the protonemal edge may be linked to the sporadic nature of caulonemal filament formation, which initially appears in seemingly random patches at the edge of the protonema (e.g. **Figure 2B**).

Mutation of either the tasiARF or the miR1219 target site results in increased *PpARFb4* expression, with a greater number of chloronemal filaments and a greater number of cells per filament showing reporter activity (**Figure 2H, I**). Consistent with the stronger phenotype of *PpARFb4-GUS-m*t** plants (**Figure 2E**), reporter activity is expanded even further upon mutation of both small RNA target sites. In these mutants, PpARFb4-GUS expressing cells occur in nearly every chloronemal filament, and expression extends further down the filament than in either the wild type, *PpARFb4-GUS-m** or *PpARFb4-GUS-t** lines (**Figure 2J**). In addition, PpARFb4-GUS levels in individual cells appear stronger than in other genotypes. Importantly, the pattern of *PpARFb4* expression in all genotypes does not change substantially from 8 to 15 or 22 days of growth, supporting the hypothesis that tasiARF and miR1219 do not establish a temporal pattern of *PpARFb* expression in protonema. Instead, the data shows that tasiARF and miR1219 act coordinately along the chloronemal filament to limit the spatial expression domain of *PpARFb4* to the outer edge of the growing protonema. Considering that *PpARFb1* and *PpARFb2* expression also increases in *Ppsgs3,* it seems likely that tasiARF and miR1219 regulate these targets similarly.

Together, these data provide a basis for the caulonemal defect of *Ppsgs3* mutants, and suggest a mechanism by which tasiARF, in concert with miR1219, regulates the chloronemal-to-caulonemal transition. Caulonema are thought to differentiate from chloronemal tip cells (Bopp,

1980). tasiARF and miR1219 regulate this process by limiting expression of PpARFb transcription factors, which act as repressors of caulonemal differentiation, to the outer edge of growing protonema. The combined activity of these small RNAs appears finely balanced such that it generates a randomly variegated pattern of PpARFb expression at the protonemal edge. In a subset of chloronemal filaments, PpARFb activity is depleted even in the tip cell, allowing their differentiation into caulonema. Upon loss of small RNA regulation, whether by disruption of tasiRNA biogenesis or small RNA complementarity within *PpARFb* transcripts, expression of these ARF proteins persists in a broader domain that encompasses a larger number of chloronemal tip cells, preventing their differentiation into caulonemal filaments. Thus, the contribution of *PpSGS3* to *Physcomitrella* gametophyte development lies primarily in the production of tasiARF and the downstream regulation of *PpARFb* genes. Interestingly, our data suggests that an absence of *PpARFb* expression is not sufficient for caulonema differentiation, as a variegated pattern of PpARFb4-GUS activity at the protonemal edge is also observed in young plants not initiating caulonemal filaments. Rather, it appears that tip cells lacking PpARFb expression are competent to differentiate into caulonema, but only do so upon receipt of a distinct signal.

tasiRNAs target repressor ARF transcripts to modulate the auxin response

ARF transcription factors, including the tasiARF targets, form part of a highly conserved GRN that regulates the response to the phytohormone auxin. This network integrates auxin perception into development by controlling the transcription of auxin-responsive genes (ARGs). ARF proteins, which have been classified as either “activator” or “repressor” based on their effect on ARG expression, bind the promoters of such genes in an auxin-independent manner. Transcription factor activity of activator ARFs is, however, blocked in the absence of auxin through dimerization with Aux/IAA proteins. The latter are degraded in response to auxin, resulting in the auxin-dependent derepression of ARG expression (Finet and Jaillais, 2012). Interestingly, the Aux/IAA genes are themselves transcribed in response to auxin signaling, forming a negative feedback loop in the auxin response GRN that is conserved between moss and flowering plants (Middleton et al., 2012; Prigge et al., 2010). The repressor ARFs add additional complexity to this network by competing with activator ARFs for binding to ARG promoters; in flowering plants, this competition between activator and repressor ARFs is thought

to allow for the differential regulation of the transcriptional auxin response in space and time (Vernoux et al., 2011).

As in flowering plants, auxin regulates a diverse set of developmental processes in moss, including those impacted by the tasiRNA pathway (Aoyama et al., 2012; Bopp, 1980; Prigge et al., 2010). Indeed, both *Ppsgs3* and lines misexpressing the *PpARFb* targets mimic phenotypes resulting from the treatment of *Physcomitrella* with the 'anti-auxin' compound p-Chlorophenoxyisobutyric acid (PCIB) (**Figure S6A, B**). The phenotypes of these mutants are also similar to those of classical auxin-insensitive mutants in moss, which form densely packed chloronema, lack caulonemal filaments, and develop fewer or no gametophores (Prigge et al., 2010). These similarities suggest that the PpARFb proteins may act as repressors of the auxin response. This hypothesis is supported by phylogenetic analysis, which places the tasiRNA-targeted *ARF*s in *Physcomitrella* sister to the 'B' group of *ARF* genes in flowering plants that includes known repressor ARFs, such as the tasiARF target *ARF3* (Plavskin and Timmermans, 2012). Indeed, consistent with a role of the *Physcomitrella* tasiRNA targets in repressing the auxin response, transcript levels of the early auxin response genes *PpIAA1a* and *PpIAA1b* (Prigge et al., 2010) are reduced in *Ppsgs3* compared to wild type (**Figure S6C**).

The role of PpARFb proteins as repressors of the auxin response provides additional insight into the stochastic nature of caulonema formation. The tasiARF- and miR1219-generated variation in PpARFb expression at the protonemal edge results in variable responsiveness of chloronemal tip cells to auxin, which is known to promote caulonemal fate. Importantly, the phenotypes of tasiRNA biogenesis mutants in flowering plants also result from changes in the spatiotemporal expression of B-group ARF genes (Chitwood et al., 2009; Dotto et al., 2014; Hunter et al., 2006; Song et al., 2012; Yifhar et al., 2012; Zhou et al., 2013). By regulating the pattern and level of repressor ARF accumulation, the tasiRNA pathway may thus act to modulate the auxin response across spatial domains in the plant; this finding sheds light on a potential ancestral function of this pathway.

Auxin regulation of *PpARFb* genes creates a second negative feedback loop in the auxin response network.

Considering the conserved role of the tasiRNA pathway in regulating canonical repressors of the auxin response, an understanding of how tasiRNAs and their targets affect the signaling properties of the ancient auxin response network at the cellular level may elucidate potential reasons for its repeated evolutionary cooption. A correct model of the architecture of the auxin response GRN is, in this regard, key. An important conserved feature of this network is the negative feedback between Aux/IAA genes and the auxin response (Prigge et al., 2010). In *Arabidopsis*, expression of a subset of repressor ARF genes is also subject to feedback from the auxin response (Marin et al., 2010; Paponov et al., 2008; Vanneste et al., 2005; Yoon et al., 2010). As this may impact a GRN's signaling properties, we determined whether auxin signaling affects expression of the *PpARFb* tasiRNA targets in *Physcomitrella* by analyzing *PpARFb1*, *2* and *4* transcript levels in plants grown on media containing 0.1 μM NAA. Transcript levels for all three genes are increased ~2.5-fold in auxin-grown plants (**Figure 3A**). Consistent with this finding, PpARFb4-GUS expression is expanded in plants grown on auxin-supplemented media, with more protonemal filaments and more cells per filament showing reporter activity (**Figure S7C, E**). Increased expression in response to auxin is also observed for the tasiRNA-resistant form of *PpARFb4-GUS* (**Figure S7D-F**), suggesting that auxin promotes *PpARFb* expression at the transcriptional level, rather than exclusively via repression of tasiARF species. Indeed, the small RNAs regulating *PpARFb* expression show a complex response to auxin treatment. Although some tasiARF species are upregulated in plants grown on media supplemented with auxin, other tasiARF species, as well as miR1219, are repressed (**Figure S4G**). These data establish the existence of a negative feedback loop between auxin and repressor *PpARFb* levels that, in addition to the highly conserved negative feedback between auxin signaling and Aux/IAA genes, modulates the *Physcomitrella* auxin response GRN. Interestingly, this network configuration appears to be partially conserved, as the *Arabidopsis* tasiARF target *ARF4* is also upregulated in response to auxin (Marin et al., 2010; Paponov et al., 2008; Vanneste et al., 2005; Yoon et al., 2010).

Repressive feedback from the tasiARF-targeted ARFs onto the auxin response may impart important properties to the auxin response GRN in *Physcomitrella.* Negative autoregulatory

circuits are central in allowing cells to buffer intrinsic noise, for example resulting from bursts of transcription of circuit components (Alon, 2007; Raser and O'Shea, 2005). However, data from flowering plants has shown that extrinsic fluctuations in auxin signaling input levels may be a significant source of noise in the auxin response GRN (Vernoux et al., 2011). To explore how the feedback loop between auxin signaling and tasiRNA-regulated ARFs affects the propagation of extrinsic auxin noise through the auxin response GRN in *Physcomitrella*, we adapted a computational model of the auxin response based on ordinary differential equations (ODEs) generated by Vernoux *et al*. (2011), and modified it to reflect the architecture of the moss auxin response GRN (**Figure 3B; Modeling Supplement**). Two important measures of GRN function, susceptibility and noise amplification, were considered with and without transcriptional regulation of repressor ARFs by auxin signaling.

Susceptibility (elsewhere also described as sensitivity or gain) measures the change in a system's output relative to a small change in input (Bintu et al., 2005; Hornung and Barkai, 2008). In this case, susceptibility reports the degree to which ARG expression changes in response to a sustained 1% change in auxin signal, and was assayed via numerical solutions of steady-state ARG transcript values.

$$\text{susceptibility} = \frac{\left([\text{IA}_{\text{TRANSCRIPT}}]_1 - [\text{IA}_{\text{TRANSCRIPT}}]_0\right) / [\text{IA}_{\text{TRANSCRIPT}}]_0}{\left(\text{Auxin}_1 - \text{Auxin}_0\right) / \text{Auxin}_0}$$

Noise amplification, on the other hand, measures the ratio between output noise and input noise (Hornung and Barkai, 2008). Here, it is indicative of the degree to which short fluctuations in auxin signaling levels (extrinsic auxin noise) are translated to fluctuations in ARG expression levels.

$$\text{noise amplification} = \frac{\sigma\left([\text{IA}_{\text{TRANSCRIPT}}]\right) / \left\langle [\text{IA}_{\text{TRANSCRIPT}}] \right\rangle}{\sigma(\text{Auxin}) / \langle \text{Auxin} \rangle}$$

Noise amplification was assayed in computer simulations of the auxin response GRN. For a detailed discussion of the modeling approach and the parameters used, see the **Modeling**

Supplement.

Feedback regulation from repressor ARFs onto the auxin response results in decreased susceptibility (**Figure SM5A**), confirming predictions made in simpler genetic networks by both theoretical work (Paulsson, 2004) and simulations (Hornung and Barkai, 2008). Unlike in the case of susceptibility, there is no clear theoretical prediction regarding the effect of negative feedback on extrinsic noise amplification (Paulsson, 2004). Our model predicts that negative feedback from the *PpARFb* genes on the auxin response minimally affects extrinsic noise amplification. The small decrease in extrinsic auxin noise amplification that is observed is not significant (**Figure SM5A**). Both findings are robust across a wide range of starting auxin input levels (**Figure S5C**), and suggest that one advantage of this network architecture may be that it can buffer intrinsic noise without imparting strong amplification of extrinsic noise. Any benefits repressive feedback regulation in the auxin response GRN has in terms of promoting robustness against intrinsic fluctuations in gene expression are, however, coupled with a loss of susceptibility.

tasiARF regulation promotes a robust auxin response

Small RNA regulation is likewise predicted to lend robustness to the output of a GRN. Indeed, a recent study showed that small RNA regulation in mammalian cells suppresses intrinsic fluctuations in target gene expression (Schmiedel et al., 2015). However, the role of small RNA regulation in modulating extrinsic noise amplification is not known. To visualize how tasiRNA regulation affects the cellular response to auxin, we simulated the output of the above auxin response network upon changes in auxin signal levels (see **Modeling Supplement**) at two repressor ARF transcript degradation rate ($\gamma_{A\text{- transcript}}$) values. The higher value, representing wild type, is based on the degradation rate of tasiRNA-targeted *ARF* transcripts in wild type *Arabidopsis* (Narsai et al., 2007). A 3.5-fold lower $\gamma_{A\text{- transcript}}$ value, which results in a change in *PpARFb* level in line with that observed in *Ppsgs3*, is used to represent a lack of tasiARF regulation. Increasing $\gamma_{A\text{- transcript}}$ resulted in a higher response output to a sustained step-increase in auxin signaling level (**Figure 3C**), reflecting increased susceptibility. In simulations of a noisy signal, increased repressor ARF transcript degradation rates resulted in larger fluctuations in auxin-regulated gene expression (**Figure 3D**). This hints at an output of the auxin response that

is more susceptible and less robust to extrinsic auxin fluctuations in the presence of tasiRNA regulation of PpARFb repressors.

However, while $\gamma_{A\text{- transcript}}$ is higher in wild type than in *Ppsgs3*, precise ARF transcript degradation rates are not known in *Physcomitrella*. We thus modeled the effect of a spectrum of $\gamma_{A\text{- transcript}}$ values on susceptibility and noise amplification. For a wide range of repressor *ARF* transcript degradation rates tested, increasing $\gamma_{A\text{- transcript}}$ results in increased susceptibility to a small, sustained auxin signal that is correlated with an increase in extrinsic noise amplification in the auxin response GRN (**Figure 3E**). Substantiating these findings, modulation of ARF translation rates ($\pi_{A\text{-}}$), which may also be affected by tasiRNA regulation, has the same linked effect on susceptibility and noise amplification levels (**Figure SM4**). In addition, these outcomes are qualitatively robust to changes in all network parameter values (see **Modeling Supplement**). This generalizes the observation that tasiRNA regulation imparts susceptibility on the auxin response that is coupled with decreased robustness to auxin input noise. However, beyond a $\gamma_{A\text{- transcript}}$ value of ~0.003, the relationship between these network properties change (**Figure 3E**). The auxin response GRN is too complex for an analysis of parameters contributing to this shift, but it is interesting to note that the best available estimates of network parameter values suggest that the wild type auxin response GRN may function close to this local maximum in susceptibility and extrinsic noise amplification.

These findings further highlight the possible multifaceted contributions of small RNA regulation to GRN properties. While simulations predict that the small RNA-mediated regulation of PpARFb repressor ARFs impairs the plants' ability to buffer ARG expression levels against fluctuations in auxin signaling input, small RNA regulation is expected to provide robustness against intrinsic noise in repressor ARF levels (Schmiedel et al., 2015). To experimentally assay the effect of tasiARF regulation on noise in the auxin response, we measured the coefficient of variance for transcript levels of six ARGs (Pires et al., 2013; Prigge et al., 2010) across biological replicates of wild type or *Ppsgs3*. Transcript levels for five of these genes, *PpIAA1a, PpIAA1b, PpIAA2, PpRSL5,* and *PpRSL6*, are more variable in *Ppsgs3* than in wild type (**Figure 3F**), and this effect is significant when measured across all six ARGs. This demonstrates that in *Physcomitrella*, the overall effect of tasiARFs on the auxin response GRN is to increase

robustness of auxin-regulated gene expression, and seems to hint at a distinct primary source of noise in the *Arabidopsis* and *Physcomitrella* auxin response GRN (Vernoux et al., 2011). As discussed above, autorepression by PpARFb genes may likewise buffer intrinsic fluctuations in the auxin response.

tasiARF regulation promotes phenotypic sensitivity to auxin

While susceptibility, which reports the change in response output resulting from a minute change in signaling input level (Bintu et al., 2005; Hornung and Barkai, 2008), is a useful measure of network signaling properties, larger changes in input levels more accurately reflect auxin signaling *in vivo* (Petersson et al., 2009). We therefore next modeled the qualitative effect of tasiRNA regulation on steady-state ARG expression across a broad range of increasing auxin signaling levels. As before, calculations were performed at two $\gamma_{A\text{- transcript}}$ values, representing wild type (high $\gamma_{A\text{- transcript}}$) and *Ppsgs3* (low $\gamma_{A\text{- transcript}}$), respectively. For both values, the output of the simulated GRN to increasing auxin-signaling levels follows a sigmoid curve. However, the ARG transcript level is lower overall in the *Ppsgs3*-like regime, with differences between the two regimes especially pronounced at high auxin signaling levels (**Figure 4A**).

To experimentally test the prediction that tasiRNA regulation sensitizes the auxin response, we measured the transcript level profiles for *PpIAA1a, PpIAA1b, PpIAA2, PpRSL1, PpRSL5,* and *PpRSL6* in wild type and *Ppsgs3* plants grown on media supplemented with between 0 - 1μM NAA (**Figure 4B-G**). Very low doses of exogenous auxin not commonly assayed were included in this range to observe the effect of subtle changes in auxin levels on ARG expression. As expected, expression of all six genes in wild type increases upon treatment with NAA. Consistent with computational predictions, the *PpIAA* gene expression profiles follow a sigmoidal curve, with the steepest increase in auxin-induced expression occurring between 0.1 and 0.3μM NAA. The change in expression for the *PpRSL* genes appears more gradual, perhaps reflecting the complex transcriptional interaction between RSL family members (Pires et al., 2013). Importantly, *Ppsgs3* plants display reduced sensitivity to auxin, as predicted by the model. Despite increased variability in transcript levels in *Ppsgs3*, significant differences between wild type and *Ppsgs3* can be observed even at low auxin levels. Transcript levels for all six ARGs are significantly upregulated in response to treatment with auxin concentrations greater than 0.1 μM

NAA, but remain lower than those seen in wild type. These results support the prediction made by our computational model that regulation of the PpARFb repressor ARFs by tasiARF results in a dramatically increased sensitivity to changes in steady-state auxin levels that promotes the auxin-dependent induction of ARGs.

The decreased sensitivity of *Ppsgs3* plants to auxin at the molecular level is reflected at the phenotypic level. As described above, 15 day-old wild type plants grown without exogenous auxin produce multiple caulonemal filaments around the circumference. The number of these filaments increases visibly in wild type plants grown on 0.01- 0.1 μM NAA, with caulonema emerging along most of the protonemal circumference upon treatment with 0.1 μM NAA (**Figure 4I-K**). On auxin concentrations beyond that, the protonemal network is increasingly comprised of caulonema, resulting in a sparser and lighter appearance (**Figure 4L, M**) In contrast, *Ppsgs3* plants grown on auxin concentrations up to 0.1 μM NAA show a minimal induction of caulonemal differentiation, and continue to form dense chloronemal networks with few or no caulonemal filaments (**Figure 4O, P**). Treatment with levels of NAA over 0.1 μM, however, can override this defect, such that caulonemal filaments differentiate along the entire protonemal circumference (**Figure 4R, S**). These findings indicate that *Ppsgs3* plants are not generally impaired in their ability to form caulonemal filaments or respond to exogenous auxin. Rather, *Ppsgs3* mutants display a reduced auxin sensitivity such that a smaller proportion of chloronemal cells differentiates into caulonema in response to a given auxin signal.

These phenotypic and gene expression data parallel the computational predictions of single-cell auxin responses and demonstrate that tasiRNAs play a key role in sensitizing the auxin response in *Physcomitrella* via their regulation of *PpARFb* genes. By spatially regulating *PpARFb* expression, tasiARFs, in concert with miR1219, create a zone of variable auxin sensitivity at the protonemal edge, allowing the ratio of caulonemal to chloronemal cells to be tuned in response to increasing auxin levels.

***Ppsgs3* plants have reduced sensitivity to environmental cues that guide development**

Quantitative regulation of development, such as that observed above in the *Physcomitrella* auxin response, is especially important in plants, which must constantly integrate a wide range of

environmental signals into their developmental programs. Caulonemal differentiation appears to be especially labile to environmental regulation, and is modulated by light quality, as well as by the levels of nutrients such as calcium, phosphorus, and nitrogen (Reski, 1998). We hypothesized that, as quantitative regulators of caulonemal differentiation, tasiARFs may play a key role in the interaction between moss and its environment. To test this possibility, we analyzed the effect that reduced substratum nitrogen has on wild type and *Ppsgs3* protonemal morphology. For wild type, decreasing nitrogen levels in the growth medium from the typical 5 mM di-Ammonium Tartrate (dAT) promotes the chloronemal-to-caulonemal transition, such that the proportion of caulonemal filaments on plants grown on media containing 1, 0.2, 0.05, or 0 mM dAT increases substantially (**Figure 5A-E**). Although the number of caulonemal filaments on *Ppsgs3* plants likewise increases with lower nitrogen levels in the media, *Ppsgs3* plants grown on 0.2 mM dAT and especially 1 mM dAT develop considerably fewer caulonema than wild type (**Figure 5F-J**), demonstrating diminished sensitivity to changes in substratum nitrogen levels. These results demonstrate that tasiRNAs are essential for allowing a sensitive developmental response to environmental cues that moss is likely to encounter in nature.

Physcomitrella's natural habitat is, however, vastly different from the agar plates on which moss is grown in the lab, and includes agricultural fields and the moist soil at the edges of bodies of freshwater (Cuming, 2011). To test how tasiRNA regulation impacts moss development in conditions more reflective of *Physcomitrella*'s natural environment, we compared the growth of wild type and *Ppsgs3* in moist soil. While it was not possible to directly observe protonemal development on soil, two months after transplantation to soil, wild type *Physcomitrella* have a central cluster of gametophores, ~2 cm wide, surrounded by many satellite gametophores (**Figure 5K, L**). By contrast, *Ppsgs3* plants have a smaller central cluster and few, if any, satellite gametophores (**Figure 5M, N**). This result suggests that the decrease in caulonemal differentiation caused by the loss of tasiRNA biogenesis severely impacts the ability of the plant to colonize its substratum, highlighting the importance of tasiRNAs in moss' interactions with its environment.

Our work shows that by spatially restricting a conserved set of *Auxin Response Factor* (*ARF*) targets to a subset of cells at the protonemal edge, tasiRNAs modulate moss' response to the

ancient phytohormone auxin. Modeling the effect of tasiARF-mediated *ARF* regulation predicts that these small RNAs alter the signaling properties of the auxin response gene regulatory network (GRN), sensitizing cells to auxin while also causing increased amplification of fluctuation in auxin signaling inputs. However, loss of tasiRNA biogenesis results in decreased robustness of auxin-regulated gene expression, likely reflecting the ability of small RNAs to buffer transcriptional noise in their targets. Loss of tasiRNA biogenesis also results in decreased auxin sensitivity, as well as decreased sensitivity to changing substratum nitrogen levels.

DISCUSSION

An ancestral role for *TAS3* tasiRNAs in modulating auxin-regulated processes via ARFb repressor proteins

Instances of repeated cooption of specific genetic networks to direct new developmental processes are common across evolution (Carroll et al., 2004a; Plavskin and Timmermans, 2012). This study considers network properties that promote recurrent cooption by investigating one often-repurposed genetic pathway, the *TAS3* tasiRNA pathway. Although this small RNA pathway likely originated in the common ancestor of all land plants (Axtell et al., 2007), its known roles in flowering plants are in a diverse set of recently evolved processes, including flower, root, and leaf development (see Plavskin and Timmermans, 2012). Our results demonstrate that in the moss *Physcomitrella patens*, the *TAS3* tasiRNA pathway acts in the gametophytic stages of development to modulate gametophore initiation, protonemal branch determinacy, and caulonemal differentiation. The roles of tasiRNAs in protonemal development likely represent an independent cooption event, rather than an ancestral function, as the extensive and complex protonemal network found in *Physcomitrella* evolved within the moss lineage (Mishler and Churchill, 1984). Nonetheless, the functional targets of the *Physcomitrella* tasiRNA pathway are conserved. Its effects on gametophyte development are via regulation of B-family repressor ARFs, whereas the functions of novel tasiRNA targets, such as the AP2- and ZF-family transcription factors (Arif et al., 2012; Axtell et al., 2007; Talmor-Neiman et al., 2006), remain unknown and are not immediately apparent from the *Ppsgs3* phenotype. Importantly, tasiRNAs in flowering plants likewise affect development via regulation of members of the B-group of

ARF genes (Chitwood et al., 2009; Dotto et al., 2014; Hunter et al., 2006; Song et al., 2012; Yifhar et al., 2012; Zhou et al., 2013). These transcription factors in turn modulate the auxin response in space and time by repressing ARG expression (Finet and Jaillais, 2012). Our findings point to an ancestral role of the *TAS3* tasiRNA pathway in modulating the auxin response, with the tasiARF-ARFb module repeatedly coopted for diverse developmental roles over the course of plant evolution.

tasiARFs promote sensitivity and robustness of the auxin response

The strong temporal fluctuations in auxin signaling levels observed in flowering plant meristems suggested that the need to buffer this extrinsic noise may be a key factor shaping the organization and evolution of the auxin response GRN (Vernoux et al., 2011). Our findings predict other properties may have driven the tasiARF-ARFb module's repeated cooption. Our model predicts that negative feedback from repressor *ARFb* genes onto the auxin response, which is at least in part conserved in flowering plants (Marin et al., 2010; Paponov et al., 2008; Vanneste et al., 2005; Yoon et al., 2010), minimally affects extrinsic noise amplification. Instead, a predicted advantage of this network feature is that it may limit intrinsic noise resulting from the inherent stochasticity of gene expression (Alon, 2007). A key contribution of the *TAS3* tasiRNA pathway to the auxin response GRN during *Physcomitrella* protonemal development may also be to confer robustness onto the auxin response, as loss of tasiRNA regulation was found to increase variation in auxin responsive gene expression. However, this contribution seems to reflect a suppression of intrinsic rather than extrinsic noise in the auxin response GRN, as our model predicts that tasiRNA regulation amplifies the extrinsic noise from fluctuating auxin signaling input levels. On the other hand, a role for small RNAs in repressing intrinsic noise is in line with recent findings in mammalian cells (Schmiedel et al., 2015). Interestingly, Schmiedel *et al.* (2015) demonstrated that intrinsic noise repression by small RNAs is especially effective when transcripts contain multiple small RNA binding sites, as is the case for the tasiRNA-targeted *ARFb* genes in moss as well as flowering plants.

The repeated repurposing of the tasiARF-ARFb module over the course of plant evolution suggests that introducing this module into a novel, auxin-regulated context may provide a

selective advantage. Both the increased sensitivity and robustness lent to the auxin response by the tasiRNA pathway promote the faithful transfer of information through a signaling network. Evidence that selection may indeed act on such network properties has been identified across the tree of life, and includes examples of selection acting on regulatory mutations that minimize expression noise in yeast (Metzger et al., 2015; Wang and Zhang, 2011), as well as the conservation of shadow enhancers that maintain robust gene expression in animal systems (Frankel et al., 2010; Hong et al., 2008). The network properties lent to the auxin response by the tasiARF-ARFb module uncovered in this work thus provide a compelling explanation for the repeated cooption of this module throughout land plant evolution. Furthermore, these signaling properties may provide an explanation for the prevalence of evolutionary conserved small RNA-target modules in plants as well as animals.

Considering these points, it is interesting to note that a subset of the flowering plant B-group *ARF* genes have lost tasiRNA regulation (Plavskin and Timmermans, 2012). Our modeling results provide a possible explanation for this diversification. As plants evolved the need to regulate auxin responses in organs where fluctuations in auxin levels are high, such as in meristems (Vernoux et al., 2011), the benefit provided by tasiRNAs in dampening intrinsic expression noise may have been offset by their amplification of extrinsic auxin input noise. Likewise, despite the apparent importance of small RNA regulation in promoting sensitivity and robustness of the auxin response, many auxin-regulated processes in *Physcomitrella* development, such as in the leafy gametophore and sporophyte (Bennett et al., 2014; Viaene et al., 2014), are unaffected when tasiRNA function is perturbed. An interesting direction for future studies may be to explore whether miR160 and its highly conserved targets in the C-family of repressor ARFs (Axtell and Bartel, 2005; Finet et al., 2012; Plavskin and Timmermans, 2012), act in place of the tasiARF-ARFb module in the regulation of these processes.

tasiARF-mediated PpARFb regulation allows for stochastic protonemal cell fate determination

In addition to the network properties acting at the cellular level, the tasiARF-mediated regulation of PpARFb expression generates stochasticity at the whole plant level. Moss protonema is a heterogenous tissue, with caulonemal filaments specified at seemingly random locations along

the edge of the protonemal network over the course of development. Well-known examples of tissues where cell fates are specified using a stochastic choice mechanism to create a randomly mixed population of cell types exist in the metazoan nervous system, and include the diversification of olfactory and visual sensory neurons (Johnston and Desplan, 2010). However, the source of stochasticity in these examples is unclear.

Our observations indicate that tasiARF, in conjunction with miR1219, regulates caulonemal fate specification in *Physcomitrella* by limiting PpARFb expression to a random subset of chloronemal tip cells. To create variability in PpARFb expression across individual filaments tips, the levels of small RNAs in the protonema must be carefully tuned. In this regard it may be interesting that in *Arabidopsis*, the cell-to-cell movement of tasiARF from a localized source creates a small RNA gradient across developing leaf primordia (Chitwood et al., 2009). A gradient of tasiARF and miR1219 activity that dissipates towards the filament tips, perhaps generated by small RNA movement from a source at the center of the protonemal network, presents a possible mechanism to generate stochastiocity in *PpARFb* expression at the protonemal edge. The fact that the number of cells expressing PpARFb varies from filament to filament can also be explained by local subtle variation in the shape of a small RNA activity gradient. If so, patterning by small RNA gradients may represent a novel mechanism of stochastic cell fate specification.

Stochastic cell fate decisions are often important for environmental plasticity, allowing 'bet-hedging' of cell fate choices within populations of cells (Johnston and Desplan, 2010). In combination with the network properties small RNA regulation confers on the auxin response GRN, stochasticity in caulonema specification resulting from spatial variation in tasiARF and miR1219 regulation of PpARFb proteins appears important for developmental plasticity. To fine-tune development in response to subtle gradations in environmental conditions, organisms must modulate development in a quantitative, graded manner. However, to create such gradation in a binary system, such as the chloronemal-caulonemal cell fate switch, cells must display variability in their response to the switch-inducing signal (Ferrell and Machleder, 1998). By limiting PpARFb expression to a random subset of chloronemal tip cells, the tasiRNA pathway, along with miR1219, creates variable auxin responsiveness at the edge of the developing protonema.

Tip cells with comparatively high small RNA activity and low repressor ARFb levels have increased auxin sensitivity, and are thus more likely to differentiate into caulonema in response to auxin signaling. Our finding that the number of caulonemal filaments increases progressively with increasing auxin levels supports this notion. The decreased response to small changes in substratum nitrogen availability in moss plants defective in tasiRNA biogenesis further underscores the importance of tasiRNAs in maintaining a plastic response to the environment.

With the role of tasiRNAs in sensitizing development to environmental inputs in mind, parallels can be drawn between independently evolved tasiRNA-regulated processes in mosses and flowering plants. Lateral root initiation in *Arabidopsis*, although likely sharing little with protonemal development in terms of cellular mechanisms, is also auxin- and tasiRNA-regulated, and is carefully tuned by environmental inputs, including substratum nitrogen levels (Gifford et al., 2008). Likewise, the auxin- and tasiRNA-regulated specification of abaxial-adaxial polarity in flowering plant leaves is sensitive to environmental inputs, with the number of adaxial and abaxial cell layers regulated in part by light quality (Kozuka et al., 2011).

Network signaling properties as drivers of GRN cooption

Although the mechanisms by which cooption of genetic networks occurs have been extensively investigated, the reasons for the preferential repeated cooption of select networks are less well understood. One potential benefit of GRN cooption is that it allows the redeployment of a 'differentiation gene battery' involved in a specific cellular or developmental process (Erwin and Davidson, 2009). For example, the *RSL* genes were repeatedly repurposed during the evolution of plant organs that develop via filamentous growth, such as protonema in moss and root hairs in flowering plants (Jang et al., 2011; Menand et al., 2007b; Pires et al., 2013). In contrast, we propose that the repeated cooption of the *TAS3* tasiRNA pathway was driven by the properties that this pathway lends to the auxin response, rather than by the redeployment of a specific downstream developmental process. We find that tasiRNAs lend the networks they regulate two key properties: robustness to intrinsic noise in target levels, and sensitivity to environmental signals. Further, small RNAs may provide a mechanism to create stochastic cell fate patterns that are developmentally plastic and increase the spectrum of responses to environmental stimuli.

Considering the signaling properties of a genetic network, and not just its developmental output, may thus be critical to understanding the evolution of complex multicellular forms.

MATERIALS AND METHODS

The transformation and propagation of *Physcomitrella* was performed as described (Cove et al., 2009a, 2009b), with minor adjustments detailed in Supplementary Materials and Methods. For phenotypic or gene expression level measurements, protonema were subcultured on cellophane plates 2-3 times, and small pieces (1-3 mm diameter) transplanted to BCDAT plates containing 0.9 μM FeSO4 at pH 5.8, unless otherwise noted. For chemical treatments, auxin, PCIB, or estradiol was added at the indicated concentrations. Nitrogen level experiments were performed on BCD plates supplemented with the appropriate amount of diammonium tartrate. For soil experiments, plants were grown on Rediearth (Sungro) under a plastic dome for two months at 22°C under a 16/8 light/dark regime. Cell size measurements were performed on chloronemal cells 3-5 cells from filament tips. Branching was analyzed on 3 week-old plants. For, gametophore counts, the number of gametophore buds with at least 1 phyllid were counted. Histochemical staining was performed on 15 day-old plants as described (Chitwood et al., 2009). For all qRT-PCR and 5' RACE experiments, total RNA was extracted from *Physcomitrella* using Trizol reagent (Invitrogen) according to the manufacturer's suggested protocol. Unless otherwise stated, RNA was extracted from whole 15 day-old plants as detailed in Supplementary Materials and Methods. Small RNA qRT-PCR was performed following a protocol modified from Varkonyi-Gasic et al. (2007), and RLM 5' RACE was performed as described in Axtell et al. (2007). All expression levels were calculated relative to untreated wild-type controls, after normalization to levels of GAPDH (gene expression) or U6 (small RNA expression). Statistical significance was calculated from at least three biological and two technical replicates using student's t-test between wild-type and mutant samples within a given condition. For detailed experimental procedures, see Supplementary Materials and Methods. For detailed computational modeling procedures, see Supplementary Modeling Information.

SUPPLEMENTARY INFORMATION

Supplementary Materials and Methods
Supplementary Figures S1 to S7

Supplementary Tables S1 and S2
Supplementary Modeling Information
Supplementary Table SM1
Supplementary Figures SM1 to SM5

ACKNOWLEDGEMENTS

We thank members of the Timmermans, Quatrano, and Hasebe laboratories who have contributed ideas and thoughtful comments to the manuscript, Tim Mulligan for plant care, and Elijah Salome-Diaz, Carol Hu, Cristina Marco, and members of the Hasebe lab for technical assistance. We also thank Teva Vernoux for sharing modeling code. YP was funded by an Al Hershey fellowship from the Cold Spring Harbor Laboratory Watson School of Biological Sciences and a predoctoral training grant 5T32GM065094 from the National Institute of General Medical Sciences. This work was also supported by the East Asia and Pacific Summer Institutes grant OISE-1015679 from the National Science Foundation and the Japan Society for the Promotion of Science. MH is funded by ERATO and KAKENHI from MEXT, Japan. Research on small RNA regulation in the Timmermans lab is supported by grants from the National Science Foundation (IOS-1355018 and MCB-1159098) and an Alexander von Humboldt Professorship from the Deutsche Forschungsgemeinschaft.

AUTHOR CONTRIBUTIONS

YP and MT conceived the study and designed the project. YP and MT planned the experiments with input from P-F.P, AN, MH, and RQ. YP, P-F.P, and AN generated the transgenic moss strains. YP performed the experiments. YP performed the computational modeling with input from GA and MT. YP and MT wrote the manuscript.

REFERENCES

Alon, U. (2007). Network motifs: theory and experimental approaches. Nat. Rev. Genet. *8*, 450–461.

Aoyama, T., Hiwatashi, Y., Shigyo, M., Kofuji, R., Kubo, M., Ito, M., and Hasebe, M. (2012). AP2-type transcription factors determine stem cell identity in the moss *Physcomitrella patens*. Development *139*, 3120–3129.

Arif, M.A., Fattash, I., Ma, Z., Cho, S.H., Beike, A.K., Reski, R., Axtell, M.J., and Frank, W. (2012). DICER-LIKE3 activity in *Physcomitrella patens* DICER-LIKE4 mutants causes severe developmental dysfunction and sterility. Mol Plant *5*, 1281-1294.

Axtell, M.J., and Bartel, D.P. (2005). Antiquity of microRNAs and their targets in land plants. Plant Cell *17*, 1658–1673.

Axtell, M.J., Snyder, J.A., and Bartel, D.P. (2007). Common functions for diverse small RNAs of land plants. Plant Cell *19*, 1750–1769.

Benkovics, A.H., and Timmermans, M.C. (2014). Developmental patterning by gradients of mobile small RNAs. Curr Opin Genet Dev *27C*, 83–91.

Bennett, T.A., Liu, M.M., Aoyama, T., Bierfreund, N.M., Braun, M., Coudert, Y., Dennis, R.J., O'Connor, D., Wang, X.Y., White, C.D., et al. (2014). Plasma membrane-targeted PIN proteins drive shoot development in a moss. Curr Biol *24*, 2776–2785.

Bintu, L., Buchler, N.E., Garcia, H.G., Gerland, U., Hwa, T., Kondev, J., Kuhlman, T., and Phillips, R. (2005). Transcriptional regulation by the numbers: applications. Curr Opin Genet Dev *15*, 125–135.

Bopp, M. (1980). The hormonal regulation of morphogenesis in mosses. In Proceedings in Life Sciences: Plant Growth Substances 1979, (Springer), 351–361.

Carroll, S.B., Grenier, J., and Weatherbee, S. (2004a). The evolution of morphological novelties. In From DNA to diversity: Molecular genetics and the evolution of animal design, Wiley-Blackwell, 159–190.

Carroll, S.B., Grenier, J., and Weatherbee, S. (2004b). From DNA to Diversity: The Primacy of regulatory evolution. In From DNA to diversity: Molecular genetics and the evolution of animal design, Wiley-Blackwell, 213–238.

Chapman, E.J., and Carrington, J.C. (2007). Specialization and evolution of endogenous small RNA pathways. Nat. Rev. Genet. *8*, 884–896.

Chitwood, D.H., Nogueira, F.T.S., Howell, M.D., Montgomery, T.A., Carrington, J.C., and Timmermans, M.C.P. (2009). Pattern formation via small RNA mobility. Genes & Development *23*, 549–554.

Cho, S.H., Addo-Quaye, C., Coruh, C., Arif, M.A., Ma, Z., Frank, W., and Axtell, M.J. (2008). *Physcomitrella patens* DCL3 is required for 22-24 nt siRNA accumulation, suppression of retrotransposon-derived transcripts, and normal development. PLoS Genet *4*, e1000314.

Cho, S.H., Coruh, C., and Axtell, M.J. (2012). miR156 and miR390 regulate tasiRNA accumulation and developmental timing in *Physcomitrella patens*. Plant Cell *24,* 4837-4849.

Cove, D.J., Perroud, P.-F., Charron, A.J., McDaniel, S.F., Khandelwal, A., and Quatrano, R.S. (2009a). Transformation of the moss *Physcomitrella patens* using direct DNA uptake by protoplasts. Cold Spring Harb Protoc *2009*, pdb.prot5143.

Cove, D.J., Perroud, P.-F., Charron, A.J., McDaniel, S.F., Khandelwal, A., and Quatrano, R.S. (2009b). Culturing the moss *Physcomitrella patens*. Cold Spring Harb Protoc *2009*, pdb.prot5136.

Cuming, A.C. (2011). Molecular bryology: mosses in the genomic era. Field Bryology *103*, 9–13.

Cuperus, J.T., Fahlgren, N., and Carrington, J.C. (2011). Evolution and functional diversification of miRNA genes. Plant Cell *23*, 431–442.

Dotto, M.C., Petsch, K.A., Aukerman, M.J., Beatty, M., Hammell, M., and Timmermans, M.C.P. (2014). Genome-wide analysis of *leafbladeless1*-regulated and phased small RNAs underscores the importance of the *TAS3* ta-siRNA pathway to maize development. PLoS Genet *10*, e1004826.

Erwin, D.H., and Davidson, E.H. (2009). The evolution of hierarchical gene regulatory networks. Nat. Rev. Genet. *10*, 141–148.

Ferrell, J.E., and Machleder, E.M. (1998). The biochemical basis of an all-or-none cell fate switch in Xenopus oocytes. Science *280*, 895–898.

Finet, C., and Jaillais, Y. (2012). AUXOLOGY: When auxin meets plant evo-devo. Dev Biol *369*, 19–31.

Finet, C., Berne-Dedieu, A., Scutt, C.P., and Marlétaz, F. (2012). Evolution of the ARF gene family in land plants: old domains, new tricks. Mol Biol Evol *30*, 45-56.

Frankel, N., Davis, G.K., Vargas, D., Wang, S., Payre, F., and Stern, D.L. (2010). Phenotypic robustness conferred by apparently redundant transcriptional enhancers. Nature *466,* 1–5.

Gifford, M.L., Dean, A., Gutiérrez, R.A., Coruzzi, G.M., and Birnbaum, K.D. (2008). Cell-

specific nitrogen responses mediate developmental plasticity. Proc Natl Acad Sci USA *105*, 803–808.

Hong, J.-W., Hendrix, D.A., and Levine, M.S. (2008). Shadow enhancers as a source of evolutionary novelty. Science *321*, 1314.

Hornung, G., and Barkai, N. (2008). Noise propagation and signaling sensitivity in biological networks: a role for positive feedback. PLoS Comput Biol *4*, e8.

Hunter, C., Sun, H., and Poethig, R.S. (2003). The *Arabidopsis* heterochronic gene *ZIPPY* is an ARGONAUTE family member. Curr Biol *13*, 1734–1739.

Hunter, C., Willmann, M.R., Wu, G., Yoshikawa, M., la Luz Gutiérrez-Nava, de, M., and Poethig, S.R. (2006). Trans-acting siRNA-mediated repression of ETTIN and ARF4 regulates heteroblasty in *Arabidopsis*. Development *133*, 2973–2981.

Jang, G., Yi, K., Pires, N.D., Menand, B., and Dolan, L. (2011). RSL genes are sufficient for rhizoid system development in early diverging land plants. Development *138*, 2273–2281.

Johnston, R.J., and Desplan, C. (2010). Stochastic mechanisms of cell fate specification that yield random or robust outcomes. Annu. Rev. Cell Dev. Biol. *26*, 689–719.

Kenrick, P., and Crane, P.R. (1997). The origin and early evolution of plants on land. Nature *389*, 33–39.

Kozuka, T., Kong, S.G., Doi, M., Shimazaki, K., and Nagatani, A. (2011). Tissue-autonomous promotion of palisade cell development by phototropin 2 in *Arabidopsis*. Plant Cell *23,* 3684-3695.

Kubo, M., Imai, A., Nishiyama, T., Ishikawa, M., Sato, Y., Kurata, T., Hiwatashi, Y., Reski, R., and Hasebe, M. (2013). System for stable β-estradiol-inducible gene expression in the moss *Physcomitrella patens.* PLoS ONE *8*, e77356.

Levine, E., McHale, P., and Levine, H. (2007). Small regulatory RNAs may sharpen spatial expression patterns. PLoS Comput Biol *3*, e233.

Marin, E., Jouannet, V., Herz, A., Lokerse, A.S., Weijers, D., Vaucheret, H., Nussaume, L., Crespi, M.D., and Maizel, A. (2010). miR390, *Arabidopsis TAS3* tasiRNAs, and their AUXIN RESPONSE FACTOR targets define an autoregulatory network quantitatively regulating lateral root growth. Plant Cell *22*, 1104–1117.

Martinez, N.J., Ow, M.C., Barrasa, M.I., Hammell, M., Sequerra, R., Doucette-Stamm, L., Roth, F.P., Ambros, V.R., and Walhout, A.J.M. (2008). A *C. elegans* genome-scale microRNA network contains composite feedback motifs with high flux capacity. Genes & Development *22*, 2535–2549.

Menand, B., Calder, G., and Dolan, L. (2007a). Both chloronemal and caulonemal cells expand by tip growth in the moss *Physcomitrella patens*. J Exp Bot *58*, 1843–1849.

Menand, B., Yi, K., Jouannic, S., Hoffmann, L., Ryan, E., Linstead, P., Schaefer, D.G., and Dolan, L. (2007b). An ancient mechanism controls the development of cells with a rooting function in land plants. Science *316*, 1477–1480.

Metzger, B.P.H., Yuan, D.C., Gruber, J.D., Duveau, F., and Wittkopp, P.J. (2015). Selection on noise constrains variation in a eukaryotic promoter. Nature *521*, 344-347.

Middleton, A.M., Farcot, E., Owen, M.R., and Vernoux, T. (2012). Modeling regulatory networks to understand plant development: small is beautiful. Plant Cell *24*, 3876-3891.

Milo, R., Shen-Orr, S., Itzkovitz, S., Kashtan, N., Chklovskii, D., and Alon, U. (2002). Network motifs: simple building blocks of complex networks. Science *298*, 824–827.

Mishler, B.D., and Churchill, S.P. (1984). A Cladistic approach to the phylogeny of the "Bryophytes." Brittonia *36*, 406.

Nagasaki, H., Itoh, J.-I., Hayashi, K., Hibara, K.-I., Satoh-Nagasawa, N., Nosaka, M., Mukouhata, M., Ashikari, M., Kitano, H., Matsuoka, M., et al. (2007). The small interfering RNA production pathway is required for shoot meristem initiation in rice. Proc Natl Acad Sci USA *104*, 14867–14871.

Narsai, R., Howell, K.A., Millar, A.H., O'Toole, N., Small, I., and Whelan, J. (2007). Genome-wide analysis of mRNA decay rates and their determinants in *Arabidopsis thaliana*. Plant Cell *19*, 3418–3436.

Nogueira, F.T.S., Madi, S., Chitwood, D.H., Juarez, M.T., and Timmermans, M.C.P. (2007). Two small regulatory RNAs establish opposing fates of a developmental axis. Genes & Development *21*, 750–755.

Paponov, I.A., Paponov, M., Teale, W., Menges, M., Chakrabortee, S., Murray, J.A.H., and Palme, K. (2008). Comprehensive transcriptome analysis of auxin responses in *Arabidopsis*. Mol Plant *1*, 321–337.

Paulsson, J. (2004). Summing up the noise in gene networks. Nature *427*, 415–418.

Petersson, S.V., Johansson, A.I., Kowalczyk, M., Makoveychuk, A., Wang, J.Y., Moritz, T., Grebe, M., Benfey, P.N., Sandberg, G., and Ljung, K. (2009). An auxin gradient and maximum in the *Arabidopsis* root apex shown by high-resolution cell-specific analysis of IAA distribution and synthesis. Plant Cell *21*, 1659–1668.

Pires, N.D., Yi, K., Breuninger, H., Catarino, B., Menand, B., and Dolan, L. (2013). Recruitment and remodeling of an ancient gene regulatory network during land plant evolution. Proc Nat Acad

Sci *110*, 9571–9576.

Plavskin, Y., and Timmermans, M.C.P. (2012). Small RNA-regulated networks and the evolution of novel structures in plants. Cold Spring Harb Symp Quant Biol *77*, 221–233.

Prigge, M.J., Lavy, M., Ashton, N.W., and Estelle, M. (2010). *Physcomitrella patens* auxin-resistant mutants affect conserved elements of an auxin-signaling pathway. Curr Biol *20*, 1907–1912.

Raser, J.M., and O'Shea, E.K. (2005). Noise in gene expression: origins, consequences, and control. Science *309*, 2010–2013.

Rensing, S.A., Fritzowsky, D., Lang, D., and Reski, R. (2005). Protein encoding genes in an ancient plant: analysis of codon usage, retained genes and splice sites in a moss, *Physcomitrella patens*. BMC Genomics *6*, 43.

Reski, R. (1998). Development, genetics and molecular biology of mosses. Botanica Acta *111*, 1–15.

Schmiedel, J.M., Klemm, S.L., Zheng, Y., Sahay, A., Blüthgen, N., Marks, D.S., and van Oudenaarden, A. (2015). MicroRNA control of protein expression noise. Science *348*, 128–132.

Skopelitis, D.S., Husbands, A.Y., and Timmermans, M.C.P. (2012). Plant small RNAs as morphogens. Curr Opin Cell Biol *24*, 217–224.

Song, X., Wang, D., Ma, L., Chen, Z., Li, P., Cui, X., Liu, C., Cao, S., Chu, C., Tao, Y., et al. (2012). Rice RNA-dependent RNA polymerase 6 acts in small RNA biogenesis and spikelet development. Plant J *71*, 378–389.

Talmor-Neiman, M., Stav, R., Klipcan, L., Buxdorf, K., Baulcombe, D.C., and Arazi, T. (2006). Identification of trans-acting siRNAs in moss and an RNA-dependent RNA polymerase required for their biogenesis. Plant J *48*, 511–521.

Vanneste, S., De Rybel, B., Beemster, G.T.S., Ljung, K., De Smet, I., Van Isterdael, G., Naudts, M., Iida, R., Gruissem, W., Tasaka, M., et al. (2005). Cell cycle progression in the pericycle is not sufficient for SOLITARY ROOT/IAA14-mediated lateral root initiation in *Arabidopsis thaliana*. Plant Cell *17*, 3035-3050.

Varkonyi-Gasic, E., Wu, R., Wood, M., Walton, E.F., and Hellens, R.P. (2007). Protocol: a highly sensitive RT-PCR method for detection and quantification of microRNAs. Plant Methods *3*, 12.

Vernoux, T., Brunoud, G., Farcot, E., Morin, V., Van den Daele, H., Legrand, J., Oliva, M., Das, P., Larrieu, A., Wells, D., et al. (2011). The auxin signalling network translates dynamic input into robust patterning at the shoot apex. Mol. Syst. Biol. *7*, 508.

Viaene, T., Landberg, K., Thelander, M., Medvecka, E., Pederson, E., Feraru, E., Cooper, E.D., Karimi, M., Delwiche, C.F., Ljung, K., et al. (2014). Directional auxin transport mechanisms in early diverging land plants. Curr Biol *24*, 2786–2791.

Wang, Z. and Zhang, J. (2011). Impact of gene expression noise on organismal fitness and the efficacy of natural selection. Proc. Natl Acad. Sci. *108,* E67–E76.

Yan, J., Cai, X., Luo, J., Sato, S., Jiang, Q., Yang, J., Cao, X., Hu, X., Tabata, S., Gresshoff, P.M., et al. (2010). The REDUCED LEAFLET genes encode key components of the trans-acting small interfering RNA pathway and regulate compound leaf and flower development in *Lotus japonicus*. Plant Physiol *152*, 797–807.

Yifhar, T., Pekker, I., Peled, D., Friedlander, G., Pistunov, A., Sabban, M., Wachsman, G., Alvarez, J.P., Amsellem, Z., and Eshed, Y. (2012). Failure of the tomato trans-acting short interfering RNA program to regulate AUXIN RESPONSE FACTOR3 and ARF4 underlies the *wiry* leaf syndrome. Plant Cell *24*, 3575–3589.

Yoon, E.K., Yang, J.H., Lim, J., Kim, S.H., Kim, S.-K., and Lee, W.S. (2010). Auxin regulation of the microRNA390-dependent transacting small interfering RNA pathway in *Arabidopsis* lateral root development. Nucleic Acids Res *38*, 1382–1391.

Zhou, C., Han, L., Fu, C., Wen, J., Cheng, X., Nakashima, J., Ma, J., Tang, Y., Tan, Y., Tadege, M., et al. (2013). The trans-acting short interfering RNA3 pathway and no apical meristem antagonistically regulate leaf margin development and lateral organ separation, as revealed by analysis of an *argonaute7/lobed leaflet1* mutant in *Medicago truncatula*. Plant Cell *25*, 4845–4862.

FIGURE LEGENDS

Figure 1: *Ppsgs3* mutants defective in tasiRNA biogenesis exhibit defects in gametophyte development. (A) Small RNA levels (mean ± SE, n ≥3) normalized to wild-type shows that in contrast to miR390, *TAS3*-derived tasiRNA levels are significantly lower in *Ppsgs3* plants than in wild-type. *P < .05; **P < .01. (B-C) Compared to wild-type (B), 15 day-old *Ppsgs3* (C) plants form drastically fewer caulonemal filaments. Dotted lines, areas at the protonemal edge lacking caulonema. Scalebar, 1mm. (D) Chloronemal cells in *Ppsgs3* filaments are shorter than in wild-type. P < 0.05; n > 20 cells. (E-F) Diagrams of branching patterns along primary filaments from 3 week-old wild-type (E) and *Ppsgs3* (F) plants shows a loss of branch determinacy in *Ppsgs3*. Diagrams show branching patterns at cells 9-18 as well as cell 29 from the tip of the primary filament. Wavy lines, cells of the main filament; numbers, cell position relative to the growing tip; red lines, primary branches; blue lines, secondary branches; yellow lines, tertiary branches; green lines, quarternary branches (white arrowhead); cyan circles, gametophore buds. Branch lengths are proportional to the number of cells in the branch. (G) Gametophore numbers (mean ± SE, n ≥6) are decreased in *Ppsgs3* compared to wild-type. *P < .05; **P < .01.

Figure 2: The *Ppsgs3* phenotype reflects misregulation of tasiARF-targeted ARFs at the protonema edge. (A) qRT-PCR values in *Ppsgs3* (mean ± SE, n ≥3) normalized to wild-type show only transcript levels of the tasiARF targets *PpARFb1*, *PpARFb2*, and *PpARFb4* are significantly increased in *Ppsgs3*. *P < .05; **P < .01; ***P < .001. (B-E) Relative to 15 day-old *PpARFb4-GUS* plants (B), which form near-normal levels of caulonemal filaments, *PpARFb4-GUS-m** (C) and *PpARFb4-GUS-t** (D) plants show a variably reduction in caulonema number, and *PpARFb4-GUS-m*t** (E) plants, with both the miR1219- and tasiARF-complementary sites mutated, only occasionally form caulonema. Dotted lines, protonemal regions lacking caulonema. Scalebar = 1mm. (F) Relative to *PpARFb4-GUS*, gametophore formation in *PpARFb4-GUS-m*t** mutants is severely delayed. Mean gametophore numbers ± SE from at least 10 plants is shown. *P < .05; **P < .01; ***P < .001. (G) In *PpARFb4-GUS* plants, reporter activity is restricted to the first 1-3 cells at tips of a small subset of chloronemal filaments. (H-J) Reporter activity is detected in more filaments and in more cells along a filament in *PpARFb4-*

*GUS-m** (H) and in *PpARFb4-GUS-t** (I). This defect is even more pronounced in *PpARFb4-GUS-m*t** (J) plants. Insets show isolated filaments; asterisks, cells expressing PpARFb4-GUS; red asterisks, tip cells. Scalebar = 0.1mm.

Figure 3: Noise-buffering properties of the auxin response GRN. (A) Transcript levels (mean ± SE, n ≥3) normalized to expression levels in plants grown on media without added NAA shows expression of *PpARFb1, PpARFb2,* and *PpARFb4* is upregulated 2-3-fold in 15 day-old plants grown on 0.1μM NAA. *P < .05; **P < .01; ***P <.001. (B) Schematic of the computational model of the *Physcomitrella* auxin response network; for details on the parameters and ODEs governing the behavior of the model, see **Table SM1** and **Equations S1-S9**, respectively. i. The model incorporates activating (ARF+) and repressing (ARF-) ARFs, as well as Aux/IAAs, which are subject to auxin-dependent degradation. ii. Aux/IAA and ARF-transcripts are produced through the activity of a promoter containing an Auxin-Responsive Element (ARE). Transcription only occurs when the promoter is bound by an ARF+ monomer or ARF+ dimer, such that the gene is repressed in all other promoter-bound states, as well as the unbound state. The activity of the promoter governs the formation of Aux/IAA and ARF-transcript. ARF- transcript degradation rate or translation rate can be increased or decreased, respectively, to simulate tasiRNA activity. (C) Simulation of ARG expression in response to a prolonged, steady auxin signaling input under both 'wild-type' and '*Ppsgs3*' conditions plotted relative to the pre-signal state, shows '*Ppsgs3*' has a lower steady-state response to an auxin input. Note the different scales used to plot auxin input and ARG expression. (D) Simulation of ARG expression in response to a noisy auxin signaling input, plotted relative to the steady-state levels of ARG expression in both 'wild-type' and '*Ppsgs3*' conditions, or relative to mean auxin level in the case of the auxin trace. The same noisy auxin signal causes smaller deviations from steady-state levels in '*Ppsgs3'* than in 'wild-type', suggesting the former may be more robust to fluctuations in auxin signaling. (E) Increasing the degradation rate of repressive ARF transcripts to reflect small RNA regulation results in increased sensitivity, but also increased noise amplification, across a large range of $\gamma_{A\text{-transcript}}$ values, followed by a small dip in noise amplification. Noise amplification shown with standard error; $\gamma_{A\text{-transcript}}$ values for 'wild-type' and '*Ppsgs3*' used in (C) and (D) are marked. (F) Loss of tasiARF regulation increases noise in ARG expression levels. Expression noise increases >2-fold in *Ppsgs3* for all ARGs tested except

PpRSL1. Across all six ARGs tested, CV is significantly higher in *Ppsgs3* than in wild-type ($P < 0.05$).

Figure 4: Perturbation of tasiRNA biogenesis dampens auxin sensitivity. (A) The model predicts steady-state ARG transcript levels, normalized to 'wild type' levels at baseline auxin signaling input, increase in both 'wild-type' and '*Ppsgs3*' and follow a sigmoid curve with increasing auxin concentrations. Final induction levels of '*Ppsgs3*' are much lower than those of 'wild-type'. The x-axis shows the value of auxin signaling input added to the baseline level in the model (see Modeling Supplement). (B-G) Relative expression (mean ± SE, n ≥3), normalized to levels in wild-type plants grown on media without added NAA, shows *PpIAA1a* (B), *PpIAA1b* (C), *PpIAA2* (D), *PpRSL1* (E), *PpRSL5* (F), and *PpRSL6* (G) transcript levels in 15 day-old wild-type and *Ppsgs3* plants increases with increasing NAA concentration and generally follows a sigmoid form. Expression of all genes increasing strongly above 0.03 – 0.1 μM NAA. *P < .05; **P < .01; ***P < .001. (H-S) 15 day-old wild-type (H-M) and *Ppsgs3* (N-S) plants grown on media supplemented with 0, 0.01, 0.03, 0.1, 0.3, or 1.0 μM NAA. In wild-type, caulonemal growth is strongly induced by NAA concentrations as low as 0.01 μM (I). As auxin concentration is increased, more and more caulonema are formed (H-M). On 0.3 μM NAA and higher, chloronema in the primary protonemal network begin to be converted into caulonema as well (L and M), as evidenced by lighter filament color; protonemal density also notably decreases. *Ppsgs3* plants grown without auxin form few or no caulonema (N). Unlike wild-type plants, caulonemal differentiation is not induced by 0.01 or 0.03 μM NAA (O-P). However, higher auxin concentrations partially rescue this defect, and *Ppsgs3* plants begin to resemble their wild-type counterparts with respect to caulonemal formation and protonemal mat density on 0.3 and 1 μM NAA (R-S). Dotted line denotes the extent of chloronemal-only filaments at the protonemal edge. Scalebar = 1 mm.

Figure 5: *Ppsgs3* has a decreased sensitivity to changes in substrate nutrient content (A-J) wild-type (A-E) and *Ppsgs3* (F-J) plants grown on BCD media supplemented with 5, 1, 0.2, 0.05, or 0 mM diAmmonium Tartrate (dAT) as an additional nitrogen source. Wild-type plants respond to decreased substrate nitrogen content by increasing caulonemal formation. Although *Ppsgs3* plants respond similarly to wild-type on media with very low levels of dAT or

without any dAT (D-E, I-J), the caulonemal response is either decreased or completely absent in *Ppsgs3* plants grown on 1 and 0.2 mM dAT (G, H). Dotted line denotes the extent of chloronemal-only filaments at the protonemal edge. Scalebar: 1mm. Concentrations labeled in terms of Ammonium ion concentrations. (K-N) Following ~2 months growth on soil, wild-type plants (K, L) often have 'satellite' gametophores away from the main plant (approximate edge of main plant highlighted with white dotted line in K and M, gametophores outside of dotted line are satellites; in schematics in L and N, circle represents position of main plant, with asterisks denoting positions of satellite gametophores). *Ppsgs3* plants (M, N) form far fewer satellite gametophores and have a more compact plant size. Scalebar: 1cm.

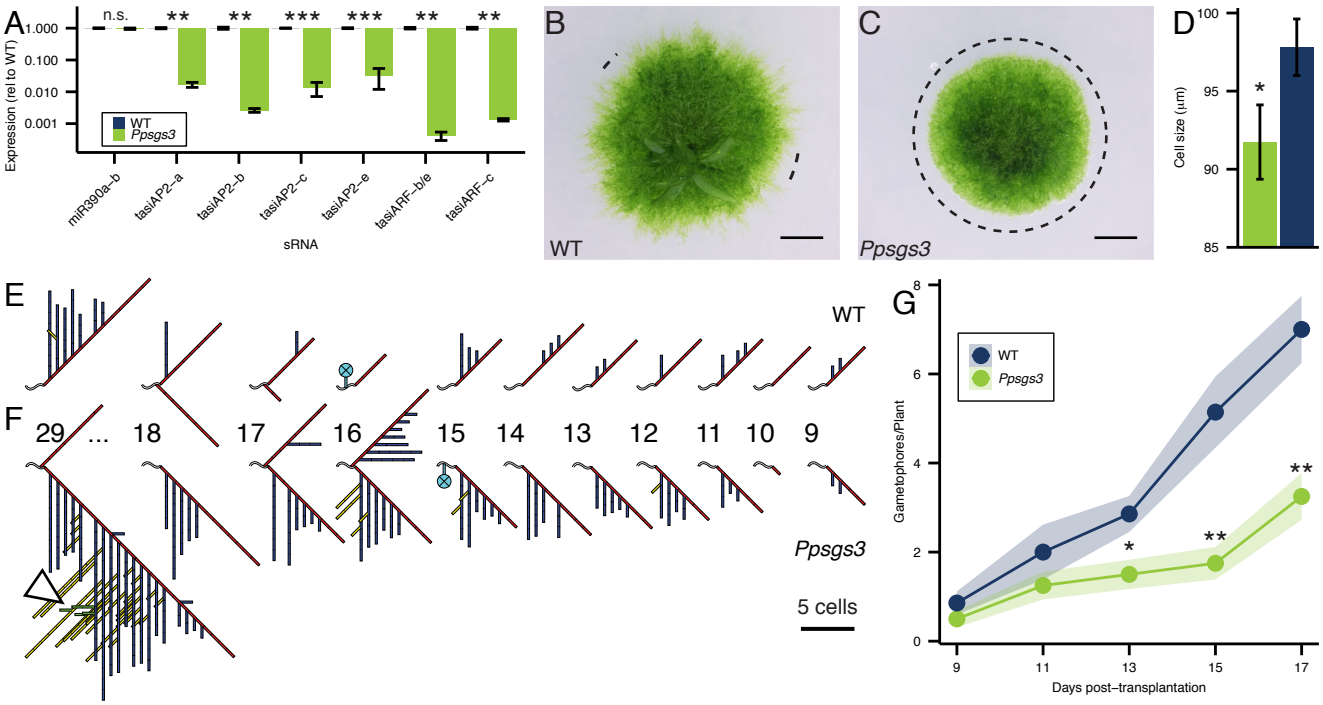
A
n.s.
**
**
***
***
**
**
1.000
0.100
0.010
0.001
Expression (rel to WT)
WT
Ppsgs3
miR390a–b
tasiAP2–a
tasiAP2–b
tasiAP2–c
tasiAP2–e
tasiARF–b/e
tasiARF–c
sRNA
B
WT
C
Ppsgs3
D
100
95
90
85
Cell size (µm)
*
E
WT
F
29
...
18
17
16
15
14
13
12
11
10
9
Ppsgs3
5 cells
G
8
6
4
2
0
Gametophores/Plant
WT
Ppsgs3
*
**
**
9
11
13
15
17
Days post–transplantation

Figure 1

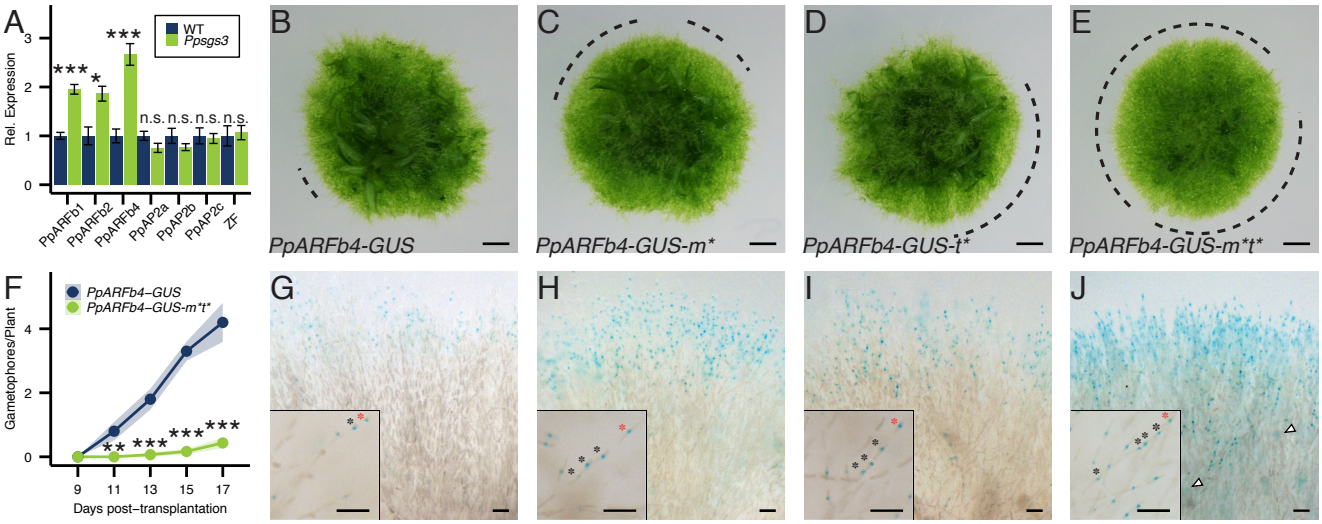
A
WT
Ppsgs3
Rel. Expression
PpARFb1
PpARFb2
PpARFb4
PpAP2a
PpAP2b
PpAP2c
ZF
B
PpARFb4-GUS
C
PpARFb4-GUS-m*
D
PpARFb4-GUS-t*
E
PpARFb4-GUS-m*t*
F
PpARFb4–GUS
PpARFb4–GUS-m*t*
Gametophores/Plant
Days post–transplantation
G
H
I
J

Figure 2

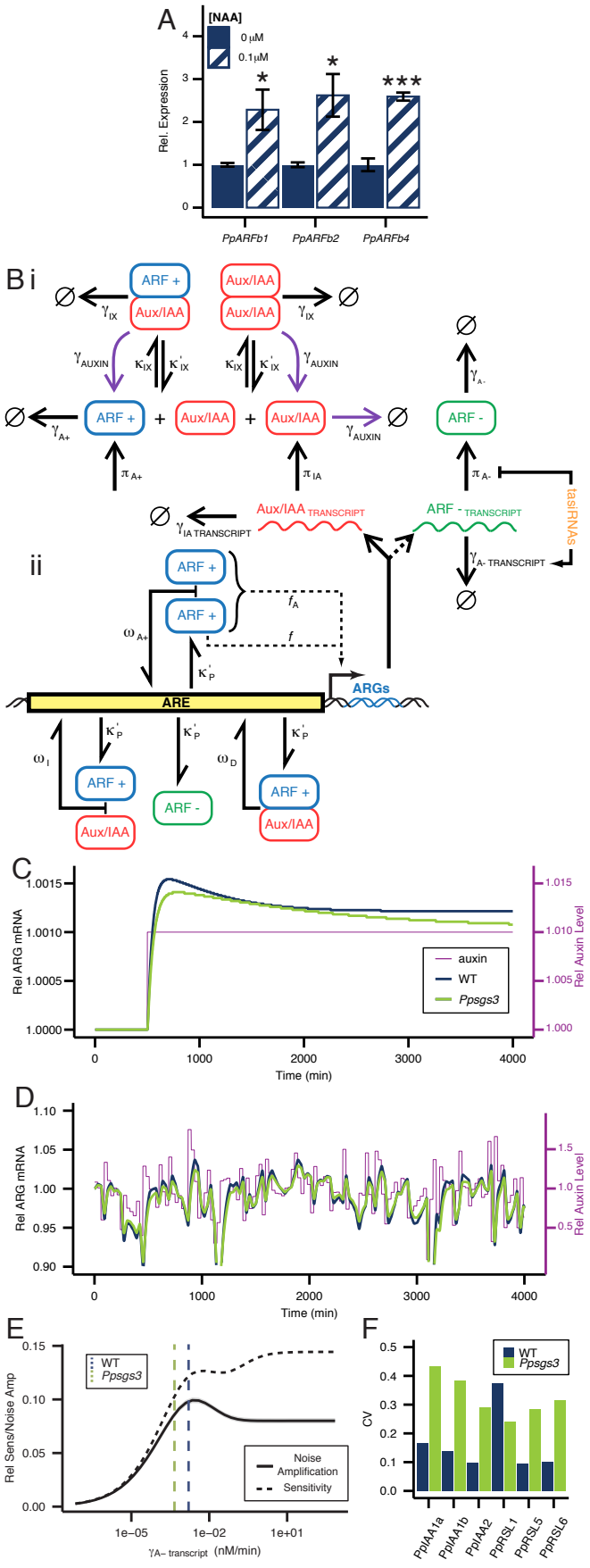
A
[NAA]
0 μM
0.1μM
Rel. Expression
PpARFb1
PpARFb2
PpARFb4
B i
ARF +
Aux/IAA
ARF -
Aux/IAA TRANSCRIPT
ARF - TRANSCRIPT
tasiRNAs
ii
ARE
ARGs
C
Rel ARG mRNA
Rel Auxin Level
auxin
WT
Ppsgs3
Time (min)
D
Rel ARG mRNA
Rel Auxin Level
Time (min)
E
Rel Sens/Noise Amp
WT
Ppsgs3
Noise Amplification
Sensitivity
γA- transcript (nM/min)
F
CV
WT
Ppsgs3
PpIAA1a
PpIAA1b
PpIAA2
PpRSL1
PpRSL5
PpRSL6

Figure 3

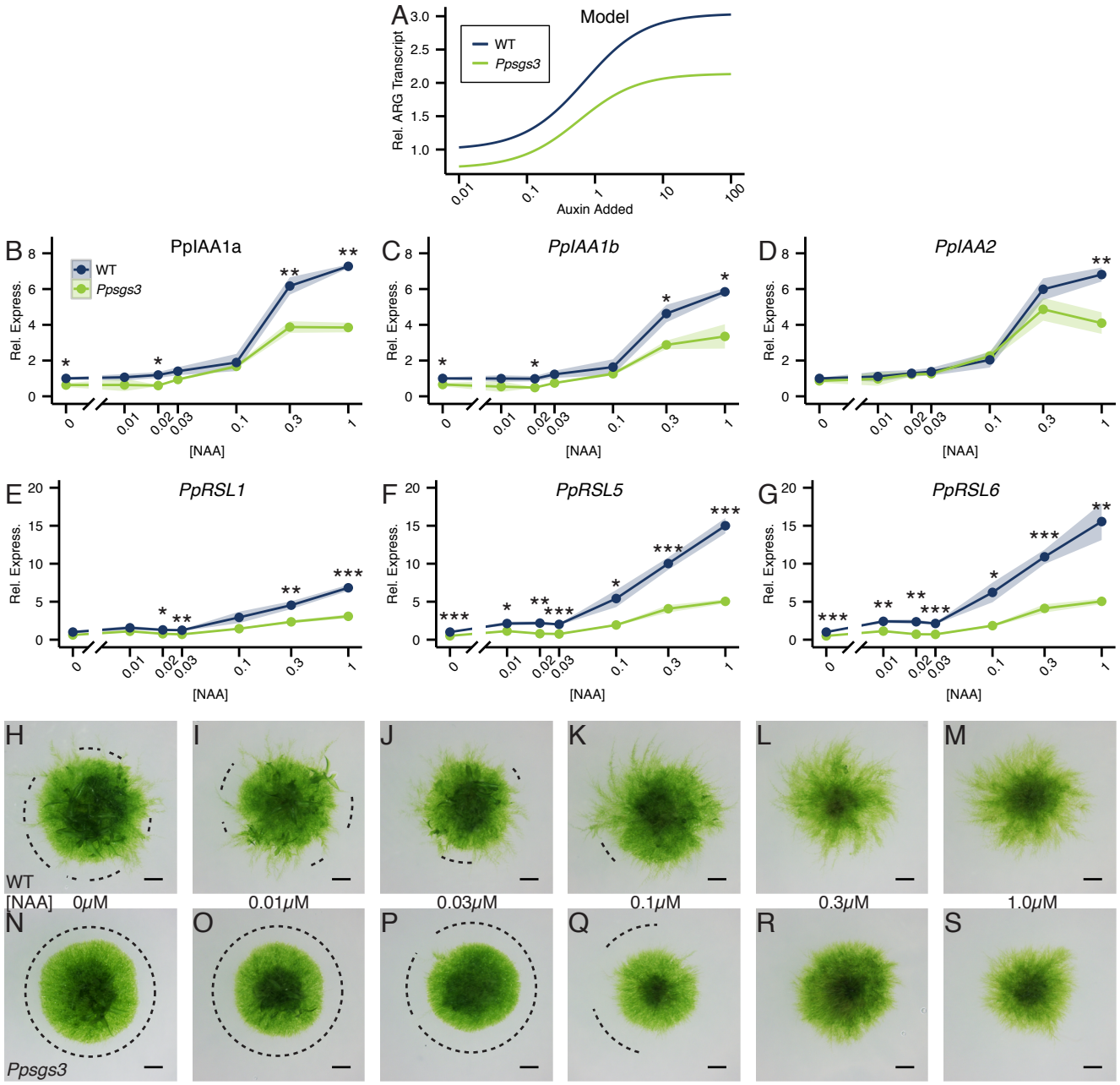
A
Model
WT
Ppsgs3
Rel. ARG Transcript
Auxin Added
B
PpIAA1a
C
PpIAA1b
D
PpIAA2
E
PpRSL1
F
PpRSL5
G
PpRSL6
Rel. Express.
[NAA]
H
I
J
K
L
M
WT
[NAA] 0μM
0.01μM
0.03μM
0.1μM
0.3μM
1.0μM
N
O
P
Q
R
S
Ppsgs3

Figure 4

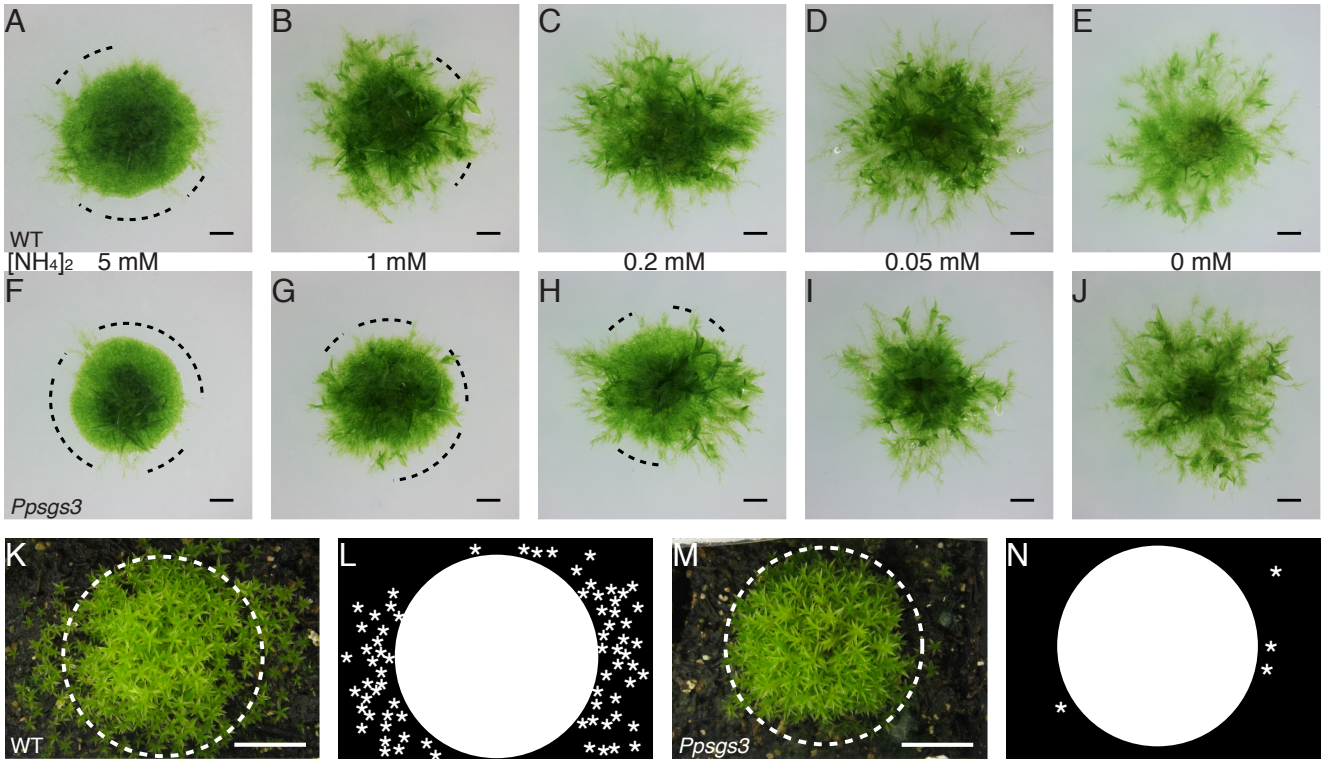
A
B
C
D
E
WT
[NH4]2 5 mM
1 mM
0.2 mM
0.05 mM
0 mM
F
G
H
I
J
Ppsgs3
K
L
M
N
WT
Ppsgs3

Figure 5